Desalination and Water Treatment
www.deswater.com

doi: 10.5004/dwt.2019.23817

151 (2019) 350–364
May

Optimization of clobetasol propionate removal by calcium peroxide using the response surface methodology

Ai Zhang[a,b], Yuye Shen[a], Xueyan Yin[a], Andere Clement Miruka[a], Yuyi Gu[c], Yanan Liu[a,*]

[a]*College of Environmental Science and Engineering, Donghua University, Shanghai 201620, China, Tel. +86 21 67792538;*
Fax: +86 21 67792522; email: liuyanan@dhu.edu.cn (Y. Liu), Tel. +86 21 67798739; Fax: +86 21 67792522;
emails: aizhang@dhu.edu.cn (A. Zhang), yuyeshen12@163.com (Y. Shen), 498707660@qq.com (X. Yin),
Tel. +86 21 67792538; Fax: +86 21 67792522; email: 418002@mail.dhu.edu.cn (A.C. Miruka)
[b]*Shanghai Key Laboratory of Atmospheric Particle Pollution and Prevention (LAP3)*
[c]*College of Environmental Science and Engineering, Beijing Forestry University, Beijing 100083, China, Tel. +86 21 67792538;*
Fax: +86 21 67792522; email: 18253489110@163.com

Received 5 September 2018; Accepted 17 January 2019

ABSTRACT

The fate of glucocorticoids (GCs) in environment has been an increasing concern. In this study, performance of calcium peroxide (CaO_2) in removing GCs was investigated using clobetasol propionate (CP) as the representative compound. Critical treatment parameters (including CaO_2 dosage, initial pH, reaction time, and initial CP concentration) were optimized for CP removal by Response surface methodology (RSM) with a four-level Box-Behnken factorial design. A coefficient of determination (R^2) value (0.97), model F-value (32.18) and its low p-value ($F < 0.0001$) along with lower value of coefficient of variation (9.35%) indicated the fitness of the model. The results showed that CaO_2 treatment was effective in CP removal due to its coupled effects of oxidation and adsorption during CaO_2 treatment. At optimum CaO_2 dosage (3.43 g L^{-1}), initial pH (7), reaction time (17.34 min), and initial CP concentration (0.03 mM), the model predicted 95.0% CP removal against the experimental value of 94.2 % CP removal. Water matrixes influenced CP removal during CaO_2 treatment in which HCO_3^- ions played an inhibitory role. The highest removal efficiency was obtained in underground water, followed by in secondary effluent, in tap water, and in surface water.

Keywords: Calcium peroxide; Clobetasol propionate (CP); Response surface methodology (RSM); Box-Behnken factorial design (BBD); Water matrix

1. Introduction

Pharmaceuticals and personal care products (PPCPs) have been detected in sewage treatment plant effluents, surface waters, groundwater, and sediments worldwide [1]. Among the PPCPs, glucocorticoids (GCs) are very important with regard to their potency [2]. GCs are a group of steroids that can affect immune system response, energy metabolism, and stress adaption in vertebrate animals [3]. They are used in treating a variety of diseases, including rheumatic, asthma, inflammatory bowel, eye and ear conditions, and inflammatory skin [1]. Depending on the therapy, type and preparation of the GC drug, the daily average dose can vary from 100 μg to 500 mg [4].

The extensive use and quick excretion of GCs have led to massive discharge of these pollutants into the environment through partially treated and untreated wastewater [5,6]. Many studies have reported the existing of GCs in environment of different areas as summarized in Table S1. Lalone et al. [7] reported that dexamethasone (Dex) was detected in river water collected downstream at a concentration of approximately 10 μg/L in France. Schriks et al.

---

* Corresponding author.

[8] found that prednisolone concentrations in hospital and industrial wastewater were 0.25 and 2 μg/L, respectively. Creusot et al. [9] detected high levels of synthetic GCs in the effluent of an industrial wastewater treatment plant (WWTP) in France with concentrations of 23 ng/L (Dex) and 300 ng/L (prednisone). Synthetic GCs in water can adversely affect fish at very low concentrations (ng/L level) [1]. Considering their high concentrations far exceeding ng/L level in the environment, synthetic GCs are highlighted as priority pollutants for future research.

Despite their high concentrations and physiological effects, to date, very few studies focus on GC removal from the environment. Most of these limited studies only investigate GC removal by sewage treatment plants (STPs) [5,10]. Unfortunately, these studies have shown that traditional treatments applied by STPs are not fully effective in eliminating these contaminants [11]. Schriks et al. [8] found that prednisolone had a relatively low removal rate (around 20%) from sewage treatment plants. Roberts et al. [12] found that the total removal efficiency for glucocorticoid potency was poorer (53%–66%) after primary and/or secondary treatment and glucocorticoid activity could persist to 4 km downstream of the effluent outfall. The low removal efficiency of GCs by STPs and their emission to environmental waters will inevitably damage aquatic organisms, and these contaminants may enter the food chain and cause adverse effects on living organisms [13]. However, no further studies have been conducted in exploring other advanced or more efficient technologies to remove GC pollutants, which is urgently required.

Advanced oxidation processes (AOPs) have drawn particular attention for degradation of endocrine disrupting compounds (EDCs) in various aqueous matrices [14–16]. Their removal efficiencies depend on chemical structures and oxidizers or ways of hydroxyl radical (HO•) generation [17]. However, research on EDCs mainly focuses on estrogenic and androgenic compounds [18]. Only a few investigations into the ability of AOPs to remove GCs have been conducted [3]. As a substitute for oxygen (O_2) and hydrogen peroxide (H_2O_2), calcium peroxide (CaO_2) was used in pollutant removal from water, soil, and sediment [18–20]. At wide pH ranges, CaO_2 dissolves in water slowly to generate H_2O_2 and O_2 (Eqs. (1) and (2)) [19].

$$CaO_2 + 2H_2O \rightarrow Ca(OH)_2 + H_2O_2 \tag{1}$$

$$2CaO_2 + 2H_2O \rightarrow 2Ca(OH)_2 + O_2\uparrow \tag{2}$$

Compared with liquid H_2O_2, solid CaO_2 releases H_2O_2 for relatively long time at a controlled rate, thus reducing H_2O_2 disproportionation, achieving higher removal efficiencies of micro-pollutants than liquid H_2O_2 [21,22]. Moreover, CaO_2 in its solid form is more stable than liquid H_2O_2, making it convenient to use, store, and transport [21]. In addition, solid forms of CaO_2 could offer active surface sites for oxidation or provide low steady-state levels of H_2O_2 for reaction with "built-in" activators and also provide an alkaline environment conducive to certain oxidation pathways [23].

Therefore, this study focused on the efficiency of CaO_2 in removing GCs. A halogenated synthetic GC, clobetasol propionate (CP), was chosen as the representative GC because of its much higher bioactivity (38 times the activity of dexamethasone) [3] and large consumption and release (top 100 most prescribed drugs in the United States) [24] among most GCs. The molecular structures and atoms label for CP are shown in Fig. 1. As most researches used traditional one-factor-at-a-time method to optimize treatment conditions in pollutant removal, the interactions of various factors were neglected [25]. In order to consider the interactions of different operational variables, response surface methodology (RSM) is created to design experimental processes evaluating effects of various variables and their interactions [26–28]. So in our study, performance of CaO_2 treatment in CP removal was evaluated by RSM. Optimum values of CaO_2 dosage, reaction time, initial pH value, and initial CP concentration have been determined by RSM for CP removal during CaO_2 treatment. The influencing mechanisms and changes of CP toxicity were tested. Influences of background water matrix constituents on effectiveness of CaO_2 treatment were also evaluated. Owing to the limited number of studies on GCs removal, to the best of our knowledge, this is the first paper using RSM to simulate CP removal during CaO_2 treatment.

2. Materials and methods

2.1. Chemicals and water matrices

The CP (Cas: 25122–46–7) standard was purchased from Sigma-Aldrich (USA). 1 g/L of CP in methanol was stored in brown bottles at 4°C. CaO_2 reagent (75%) and humic acid (HA, > 90%) was purchased from Aladdin Reagent Co. Ltd. (Shanghai, China). Inorganic chemicals (including sodium hydroxide (NaOH) and sulfuric acid (H_2SO_4)) were of analytical grade and were purchased from Sinopharm Chemical Reagent (Shanghai, China). Organic solvents (including methanol, acetic acid, and acetonitrile) were of high-performance liquid chromatography (HPLC) grade and were obtained from Sigma-Aldrich. Ultrapure water was achieved from a Milli-Q water process (Classic DI, ELGA, Marlow, UK).

In addition, four real water samples were collected in order to evaluate the influence of water matrix: the tap water (TW) collected from the lab in Shanghai (N 31°3′39″;

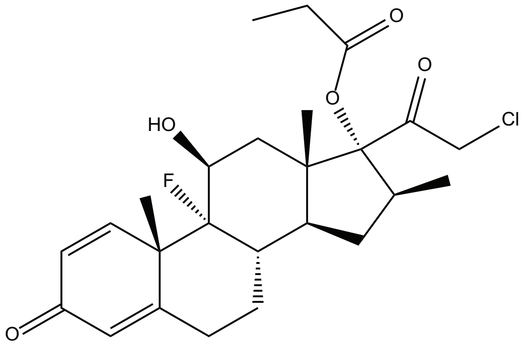

Fig. 1. Chemical structure of clobetasol propionate.

E 121°12′21′′); the underground water (UW) collected from Chengdu, south-west of China (N 30°42′37′′; E 103°50′28′′); the surface water (SW) collected from a lake in Shanghai (N 31°3′30′′; E 121°12′18′′); the secondary effluent (EW) collected from a wastewater treatment plant, also in Shanghai (N 31°17′10′′; E 121°29′34′′). These water samples were vacuum-filtered through 0.45 μm nitrocellulose filters before use. The water quality parameters were tested and are shown in Table 1.

2.2. Experimental procedures

Experiments were performed in 1 L of brown bottles magnetic stirring at room temperature. Desired CP was added to the bottle and then the solution in bottle was blown with nitrogen (N_2) to reduce the methanol. The initial pH was controlled by appropriate amount of NaOH or H_2SO_4. After adjusting the pH, calculated amount of CaO_2 reagent was added to the solution to initiate the reaction. At desired time intervals, samples were withdrawn and transferred to 150 mL brown bottles. Excess $Na_2S_2O_3$ were added to the bottles of 150 mL immediately to quench the reaction. Then the solutions in bottles of 150 mL were filtered and analyzed.

2.3. Experimental design and statistical model

The Box-Behnken factorial design (BBD) was used to evaluate the performance of CaO_2 for CP removal and optimized the operational conditions [29]. For CP removal efficiency during CaO_2 treatment in an aqueous solution, four factors (i.e., CaO_2 dosage (g L^{-1}), initial pH value, reaction time (min), and initial CP concentration (mM)) were investigated by RSM. For statistical calculations, the four factors were designated as X_1 (CaO_2 dosage (g L^{-1})), X_2 (initial pH value), X_3 (reaction time (min)), and X_4 (initial CP concentration (mM)), respectively, and were coded according to Eq. (3):

$$x_i = \frac{X_i - X_0}{\Delta X_i} \tag{3}$$

Table 1
Physical and chemical properties of different water matrix

Quality	Water matrix			
	TW	UW	SW	EW
pH	7.65	7.4	7.94	7.8
Temperature (^{o}C)	20.8	21.5	20.8	21.4
Conductivity (us/cm)	452.5	13.9	565.3	605.4
TOC (mg/L)	7.1	5.7	11.6	12.6
Cl^- (mg/L)	192.7	2.2	181.9	1165.5
SO_4^{2-} (mg/L)	53.3	0.5	67.1	24.6
HCO_3^- (mg/L)	103.7	12.2	170.2	100.7
NO_3^- (mg/L)	5	0.8	8.6	7.7
Mg^{2+} (mg/L)	7.85	0.15	11.99	10.41
Fe^{2+} (mg/L)	9.37	1.43	5.66	13.52
Na^+ (mg/L)	32.19	0.69	40.89	41.27
Ca^{2+} (mg/L)	33.14	1.14	43.52	39.18

where x_i is the coded value of an independent variable, X_i is the real value, X_0 is the real value at the centre point and ΔX_i is the step change value [30]. The lowest level (–1) of the variables and highest levels (+1) of the variables for the BBD design were CaO_2 dosage 0.05 and 4 g L^{-1}, initial pH 2 and 12, reaction times were 0.5 and 18 min, and initial CP concentrations of 0.02 and 0.06 mM as shown in Table 2. The CP removal efficiency was multiply-regressed with regard to the different parameters by the least square methods as shown in Eq. (4):

$$Y = \beta_0 + \sum \beta_i x_i + \sum \beta_{ij} x_i x_j + \sum \beta_{ii} x_i^2 \tag{4}$$

where Y is the predicted response variable (CP removal efficiency); β_0, β_i, β_{ii}, and β_{ij} are constant regression coefficients of the model; x_i and x_j (i = 1– 4; j = 1–4, $i \neq$ j) represent the variables in the form of coded values.

For BBD, the number of experimental runs (N) is given by $N = 2k(k–1) + C_0$, where k is the number of variables and C_0 is the number of center points [29]. There were 29 runs for the BBD design in our study as shown in Table 3. All the 29 runs were conducted at random order with two replicates. The quantitative relationship between the CP removal efficiency and different levels of variables was obtained by Box-Behnken design using the software (Design Expert software version 8.0.6, Stat ease). According to effects of each variable, optimum value of each variable was recommended by the software to achieve maximum CP removal efficiency.

2.4. Effects of water matrix on CP removal

The effects of inorganic ions (Cl^-, HCO_3^-, SO_4^{2-}, NO_3^-) on CP removal were investigated in ultrapure water at ion concentrations of 1, 10, and 100 mM at unadjusted pH, CaO_2 of 3.43 g L^{-1}, CP at 0.03 mM, and reaction time for 10 min. Effects of HA on CP removal were tested in ultrapure water at HA concentration of 0.1–2 g L^{-1} at unadjusted pH, CaO_2 of 3.43 g L^{-1}, CP at 0.03 mM, and reaction time for 10 min. The removal efficiencies of CP in various real water matrixes were determined at unadjusted pH, CaO_2 of 3.43 g L^{-1}, CP at 0.03 mM, and reaction time for 18 min.

2.5. Analytical methods

2.5.1. Analysis of CP

For CP analysis, 100 mL of water sample was enriched and purified by solid phase extraction (SPE) as described in the article written by Jia et al. [3]. The extract was dried by

Table 2
Range of variation of parameters used in the Box-Behnken design

Factors	Levels		
	–1	0	+1
CaO_2 dosage (X_1, g/L)	0.05	2.02	4.00
Initial pH (X_2)	2.00	7.00	12.00
Reaction time (X_3, min)	0.50	9.25	18.00
Initial CP concentration (X_4, mM)	0.02	0.04	0.06

Table 3
Box-Behnken design matrix in coded terms along with experimental and predicted values for CP removal efficiency

Runs	Independent variables (coded)				CP removal efficiency (%)		Residues
	x_1	x_2	x_3	x_4	Experimental	Predicted	
1	–1	0	1	0	30.0	26.2	3.8
2	0	1	–1	0	58.4	56.8	1.6
3	0	1	0	1	83.3	80.5	2.8
4	1	0	–1	0	35.2	37.8	–2.6
5	0	1	1	0	86.2	91.0	–4.8
6	1	0	0	1	61.0	57.9	3.1
7	0	–1	0	–1	41.5	43.0	–1.5
8	–1	0	–1	0	32.1	32.3	–0.2
9	–1	1	0	0	44.7	44.3	0.4
10	0	0	–1	–1	44.2	46.2	–2
11	0	0	0	0	70.0	70.0	0
12	1	0	0	–1	83.8	80.9	2.9
13	1	0	1	0	90.6	89.2	1.4
14	0	–1	0	1	40.4	43.8	–3.4
15	–1	0	0	1	43.6	47.7	–4.1
16	0	1	0	–1	83.8	79.1	4.7
17	–1	0	0	–1	18.3	22.6	–4.3
18	1	1	0	0	80.0	84.5	–4.5
19	0	0	0	0	63.0	70.0	–7
20	0	0	–1	1	54.5	54.9	–0.4
21	0	0	1	–1	76.8	76.3	0.5
22	0	0	0	0	74.8	70.0	4.8
23	0	0	0	0	78.3	70.0	8.3
24	0	–1	–1	0	35.6	32.0	3.6
25	0	0	1	1	72.0	69.9	2.1
26	0	–1	1	0	40.2	43.0	–2.8
27	1	–1	0	0	41.8	42.1	–0.3
28	0	0	0	0	63.9	70.0	–6.1
29	–1	–1	0	0	18.4	13.8	4.6

nitrogen and was dissolved in 1 mL of methanol for HPLC analysis with a C–18 column (4.6 × 250 mm, 5 µm) obtained from Agilent, USA. The wavelength for UV detection was set at 240 nm. The solvent program for mobile phase is described in Table 4 using acetonitrile and water. The quantification limit of CP for this method was 0.147 µM. The recoveries for CP were in range of 94%–102%.

2.5.2. *Analysis of surface properties of CaO_2 particles*

Experiments investigating interaction effects between CaO_2 particles and CP molecules were conducted in 1 L of brown bottles where the initial CP concentration was 0 and 0.6 mM, respectively. CaO_2 reagents of 0.1 g L^{-1} were added with pH unadjusted. After stirring for 1 min, the solutions were filtered. The residuals on the filters were freeze-dried and investigated by scanning electron microscopy (SEM) equipped with energy dispersive spectroscopy (EDS; FEI Quanta 200). The CaO_2 surface area and the residuals were achieved by Brunauer-Emmett-Teller (BET) analysis with a Beckman Coulter 3100 pore size and surface area analyzer.

Table 4
The detailed mobile phase gradient for CP analysis

Time (min)	Acetonitrile (%)	Water (%)
0	28	72
3	28	72
4	60	40
8	70	30
8.5	100	0
10	100	0

2.5.3. *Analysis of UV absorbance*

Scans of the UV absorbance of the CP samples during CaO_2 treatment were performed at specific sampling times (0, 2, 4, 8, and 12 min). A UV visible spectrophotometer (Cary 50 Conc, Varian, USA) was used for the scan. The wavelengths for the scan were ranging from 210 to 280 nm. For CaO_2 treatment, the initial pH was 7 and the initial CP concentration was 0.06 mM with a CaO_2 dosage of 0.08 g L^{-1}.

2.5.4. Analysis of properties of real water matrices

Upon sample receipt, water quality parameters were measured. The pH and temperature were measured with a pH meter (FE28, Mettler Toledo); the conductivity was detected using a conductivity meter (3020M, Jenco, USA); total organic carbon (TOC) was determined using a TOC analyzer (TOC-V CPH, Shi-madzu, Tokyo, Japan); the anion analysis (including Cl^-, SO_4^{2-}, HCO_3^-, and NO_3^-) was achieved by the IC25 ion chromatography system (Thermo Scientific, CA). An inductive coupled plasma emission spectrometer (ICP, Agilent 720ES) was used to analyze the metal ions.

3. Results and discussion

3.1. Development of regression model equation and validation of the model

As shown in Table 3, variation of selected factors (CaO_2 dosage, initial pH, reaction time, and initial CP concentration) greatly affected CP removal efficiency during CaO_2 treatment. According to Eq. (4), the data in Table 3 were analyzed by multiple regression analysis. The predicted response Y_m for CP removal efficiency (%) was achieved as shown in Eq. (5):

$$\begin{aligned} Y_m = {} & 69.99 + 17.12x_1 + 18.21x_2 + 11.31x_3 \\ & + 0.54x_4 + 2.98x_1x_2 + 14.38x_1x_3 - 12.02x_1x_4 \\ & + 5.80x_2x_3 + 0.13x_2x_4 - 3.78x_3x_4 - 16.58x_1^2 \\ & - 7.22x_2^2 - 7.04x_3^2 - 1.11x_4^2 \end{aligned} \tag{5}$$

In Eq. (5), Y_m is the CP removal efficiency (%); x_1, x_2, x_3, and x_4 are the influencing factors in coded units, that is, CaO_2 dosage, initial pH value, reaction time, and initial CP concentration, respectively.

In order to ensure the adequacy of the model, ambiguous results were avoided by the analysis of variance (ANOVA) and "t-test" [31,32]. As shown in Table 5, the model obtained, as shown in Eq. (3), was significant. As indicated in Table 5, the model's F-value is 32.18 with a low probability value ("Prob > F") below 0.0001. This implied that the model was significant for CP removal efficiency. There was only 0.01% chance that a "Model F-value" could occur due to noise [31]. Similarly, the adequate precision (AP) could also evaluate the signal-to-noise ratio. The desired value of AP is 4 or more [26–28]. The AP of the model for CP removal efficiency is 20.215, indicating a good fit of the model. Besides, the R^2 value for this model was 0.9699 as shown in Table 5, indicating the fit of the model in navigating the design space for CP removal efficiency [33]. Therefore, the regression model in our study explained well the CP removal during CaO_2 treatment for these response variables (CaO_2 dosage, initial pH, reaction time, and initial CP concentration). The ANOVA analysis for the RSM model gave F-value of 32.18, *p*-value of < 0.0001, AP ratio of 20.215, and R^2 value of 0.9699, signifying that the model (shown as Eq. (3)) was accurate and the experimental data are reliable (Table 5).

Significance of each coefficient in Eq. (5) is listed in Table 5. The coefficient is significant if its *p*-value is less than 0.05. As shown in Table 5, the linear effect of coefficients CaO_2 dosage ($p < 0.0001$), initial pH value ($p < 0.0001$), and reaction time ($p < 0.0001$) was significant. The interactive effects

Table 5
Analysis of variance (ANOVA), regression coefficient estimate and test of significance for CP removal efficiency (response surface quadratic model)

Factor	Sum of squares	d.f.	Mean square	Coefficient estimated ± S.E.	*F*-value	*p*-value Prob> *F*	
Model	12704.11	14	907.44	+69.99 ± 2.37	32.18	<0.0001	Significant
x_1	3516.45	1	3516.45	+17.12 ± 1.53	124.70	<0.0001	Significant
x_2	3979.61	1	3979.61	+18.21 ± 1.53	141.12	<0.0001	Significant
x_3	1536.12	1	1536.12	+11.31 ± 1.53	54.47	<0.0001	Significant
x_4	3.46	1	3.46	+0.54 ± 1.53	0.12	0.7315	
x_1x_2	35.46	1	35.46	+2.98 ± 2.66	1.26	0.2810	
x_1x_3	827.14	1	827.14	+14.38 ± 2.66	29.33	<0.0001	Significant
x_1x_4	578.16	1	578.16	–12.02 ± 2.66	20.50	0.0005	Significant
x_2x_3	134.33	1	134.33	+5.80 ± 2.66	4.76	0.0466	Significant
x_2x_4	0.063	1	0.063	+0.13 ± 2.66	0.00	0.9631	
x_3x_4	57.08	1	57.08	–3.78 ± 2.66	2.02	0.1767	
x_1^2	1782.38	1	1782.38	–16.58 ± 2.09	63.21	<0.0001	Significant
x_2^2	338.16	1	338.16	–7.22 ± 2.09	11.99	0.0038	Significant
x_3^2	321.74	1	321.74	–7.04 ± 2.09	11.41	0.0045	Significant
x_4^2	8.05	1	8.05	–1.11 ± 2.09	0.29	0.6015	
Residual	394.79	14	28.20				
Lack of fit	217.15	10	21.72		0.49	0.8364	Not significant
Pure error	177.64	4	44.41				
Corrected total	13098.90	28					

AP = 20.215, R^2 = 0.9699, Adj. R^2 = 0.9397, Pred. R^2 = 0.8833, and C.V. = 9.35 %.

of CaO_2 dosage and reaction time ($p < 0.0001$), CaO_2 dosage and initial CP concentration ($p < 0.0005$), initial pH value and reaction time ($p < 0.0466$) were also significant. The effects of the quadratic terms CaO_2 dosage (x_1^2) ($p < 0.0001$), initial pH values (x_2^2) ($p < 0.0038$), and reaction time (x_3^2) ($p < 0.0045$) were significant. Small variations of these significant variables could sharply change the CP removal efficiency.

The final regression model in terms of actual factors for CP removal is expressed by Eq. (6):

$$\begin{aligned} Y_1 = & -33.84 + 28.24x_1 + 5.80x_2 + 1.25x_3 + 1056.91x_4 \\ & + 0.30x_1x_2 + 0.83x_1x_3 - 304.37x_1x_4 + 0.13x_2x_3 \\ & + 1.25x_2x_4 - 21.58x_3x_4 - 4.25x_1^2 - 0.29x_2^2 \\ & - 0.092x_3^2 - 2785.21x_4^2 \end{aligned} \tag{6}$$

subjected to CaO_2 of 0.05–4 g L^{-1}, pH of 2–12, reaction time of 0.05–18 min, and CP concentration of 0.02–0.06 mM.

Table 3 gives the experimental values and predicted values for CP removal efficiency calculated by Eq. (6). The predicted values for CP removal efficiency were close to the experimental ones as shown in Fig. 2.

Besides predicted values, the model residuals, the internally studentized residuals, and Box-Cox transform of power were also evaluated as shown in Fig. 3. As shown in Fig. 3(a), the residuals lie approximately along a straight line, showing that the residuals were normal [34]. As shown in Fig. 3(b), there were no series of increasing or decreasing residuals with increasing fits, indicating that the model was reliable [34]. As shown in Fig. 3(c), the residuals vs. run outlier points were found to be inside the red lines, which meant that the model was well fitting [35]. In Box-Cox plots (Fig. 3(d)), the observed lambda value was 1, indicating that

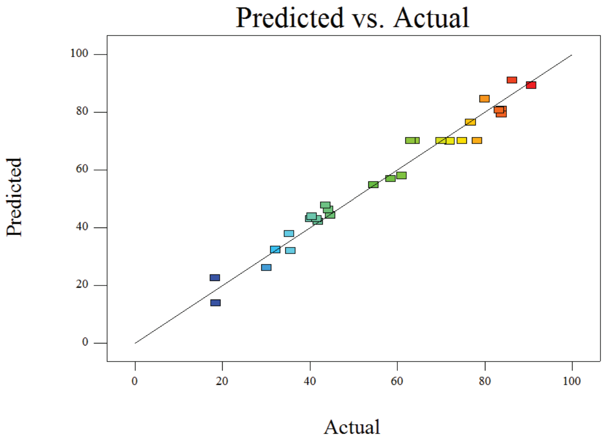

Fig. 2. Actual vs. predicted values for the response of CP removal efficiency.

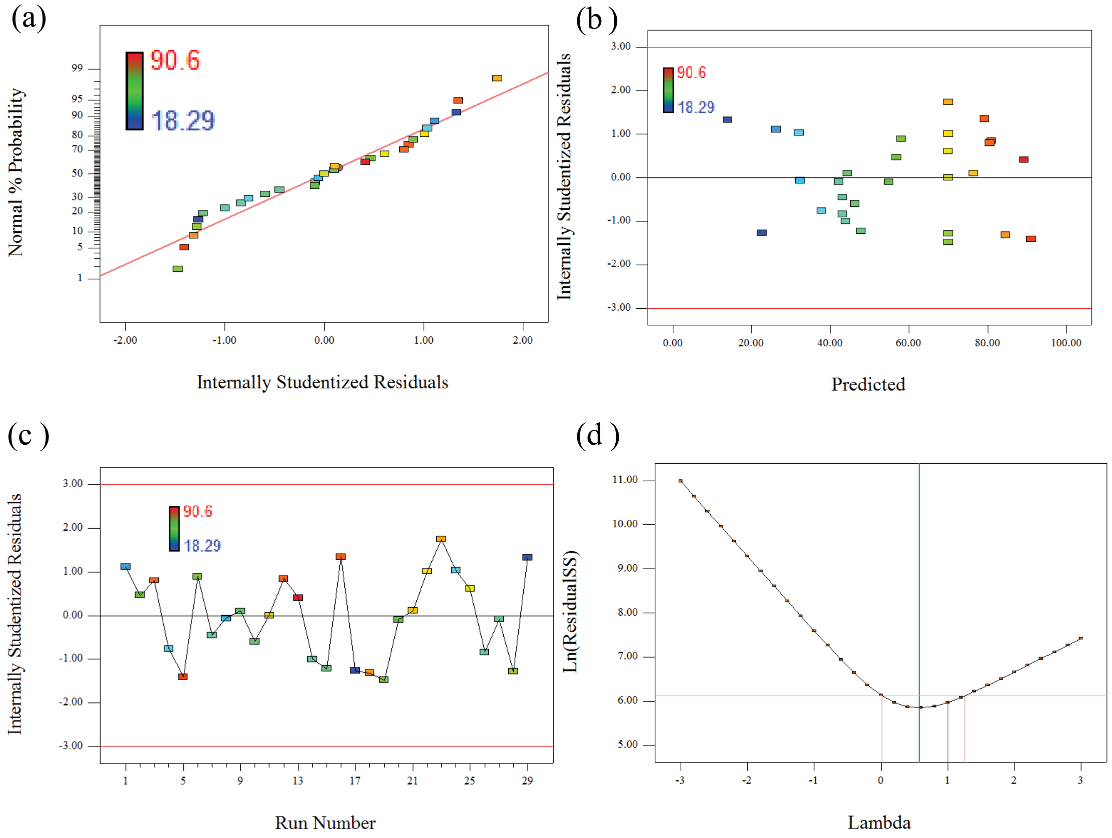

Fig. 3. Plots for diagnostics studies of the model for optimization of CP removal efficiency. (a) Plots of normal probability vs. internally studentized residuals, (b) plots of internally studentized residuals vs. predicted values, (c) plots of internally studentized residuals vs. run number, (d) Box-cox plots for power transformation.

no transformation was required [35]. So The RSM model developed in this study could be used to predict CP removal during CaO_2 treatment and navigate the practical treatment by CaO_2.

3.2. Effects and interactions of different variables on CP removal efficiency

3.2.1. CaO_2 dosage and reaction time

As shown in Figs. 4(a) and (b), the response surface and contour plot for CaO_2 dosage and reaction time were achieved at initial pH value of 7 (central level) and initial CP concentration at 0.04 mM. CP removal efficiency reached 80% at initial CP concentration of 0.04 mM and initial pH at 7, when reaction time was above 14.5 min and CaO_2 dosage was higher than 2.82 g L^{-1}. This shows that CaO_2 treatment is an effective technology in removing CP.

With CaO_2 dose increased, CP removal efficiency increased at first and then decreased slightly, especially at short reaction time. The reason can be explained by the generation of hydroxyl radicals (HO•) during CaO_2 treatment. With the increase of CaO_2 dosage, more H_2O_2

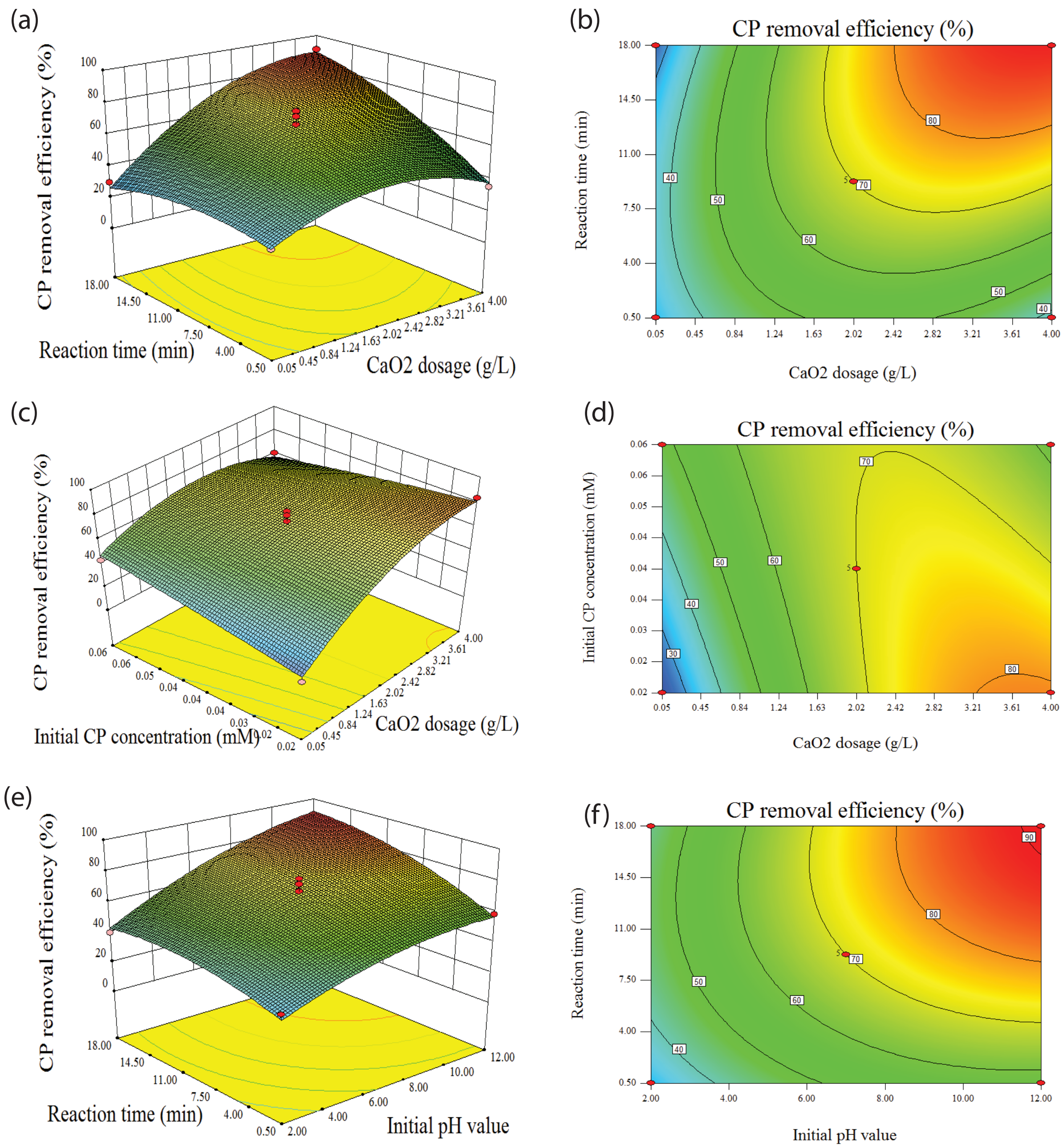

Fig. 4. Response surface plots (a, c, and e) and contour plots (b, d, and f) for effects of the CaO_2 dosage and reaction time (a and b), CaO_2 dosage and initial CP concentration (c and d), and initial pH value and reaction time (e and f) on CP removal efficiency while the other variables kept at central level.

released [(shown in Eq. (1)], promoting the CP removal. However, further increase in the CaO_2 dosage generated excessive H_2O_2. On the contrary, the excess H_2O_2 would scavenge HO• radicals as shown in Eqs. (7) and (8) [36]:

$$H_2O_2 + HO\bullet \rightarrow H_2O + O_2^{-}\bullet \tag{7}$$

$$HO\bullet + HO\bullet \rightarrow H_2O_2 \tag{8}$$

The increase in CaO_2 dosage therefore, does not guarantee better performance in CP removal during CaO_2 treatment.

It is also clear from Figs. 4(a) and (b) that the reaction time has positive effects on CP removal efficiency. This trend became more obvious at higher CaO_2 dosages. The reason can be explained using Eqs. (1) and (9) [37]:

$$2H_2O_2 \rightarrow O_2 + 2H_2O \tag{9}$$

CaO_2 is a controlled-release reagent, it dissolves in water slowly and generate H_2O_2 continuously. With the increase of the reaction time, more CaO_2 was dissolved and more H_2O_2 was released. This meant that more HO• radicals were released to oxidize CP, causing higher CP removal efficiencies.

In Fig. 4(b), an interaction between the CaO_2 dosage and reaction time occurred. Generally, a circular contour of response surfaces indicates no interaction while an elliptical or saddle nature of the contour plots indicates that the interaction is significant [38]. As can be seen in Fig. 4(b), interactions between CaO_2 dosage and reaction time were so significant that showed a clear elliptical nature of the contour plot. The joint effect of CaO_2 dosage and reaction time caused a clear curvature and a distinguished peak as shown in Fig. 4(a).

3.2.2. CaO_2 dosage and initial CP concentration

The surface response and contour plots of CaO_2 dosage and initial CP concentration are shown in Figs. 4(c) and (d) with the reaction time and initial pH value kept at central levels. At CaO_2 dosage of less than 2.02 g L^{-1}, the initial CP concentration had positive effects on CP removal efficiency. Higher CP concentration facilitated the reaction of CP with H_2O_2 released by CaO_2. The release of H_2O_2 also facilitated simultaneous dissolution of CaO_2, thus promoting the CP removal.

However, at a CaO_2 dosage larger than 2.42 g L^{-1}, the initial CP concentration has negative effects on CP removal efficiency. This trend became much more obvious at higher initial CP concentration. A considerable drop of CP removal efficiency occurred in CaO_2 dosage of more than 2.82 g L^{-1} and CP concentration larger than 0.04 mM. As shown in Figs. 4(c) and (d), the interactions were so significant that it showed clear curvature in the three-dimensional surface and saddle nature of the contour plot. As can be seen in Table 5, the joint effect of CaO_2 dosage and initial CP concentration had a negative effect on CP removal with a negative coefficient of $x_1 x_4$ (–12.02 ± 2.66). To explain the obvious negative interactions of CaO_2 dosage and initial CP concentration to CP removal at high variable levels, surface properties of CaO_2 were researched by characterizing the surface morphology of CaO_2 particles with and without the addition of high concentration of CP (Fig. 5).

As shown in Figs. 5(c)–(f), the SEM images indicate porous and semispherical flaky shape CaO_2 particles without the addition of CP (Figs. 5(c)–(e)). However, the CaO_2 particles were agglomerated with the addition of CP (Figs. 5(d) and (f)). The surface area of CaO_2 particles decreased sharply because of aggregation. As shown in Figs. 5(a) and (b), the surface areas of CaO_2 particles before and after the addition of CP were determined by N_2 adsorption-desorption isotherms and BET curves. The results showed that the surface area of CaO_2 decreased after CP addition. The specific surface area characteristic was one of the main parameters affecting the activity of CaO_2 reagent due to provision of available sites for adsorption of pollutants and/or production of reactive species [39]. So the decrease of surface area of CaO_2 at high CP concentration and CaO_2 dosage weakened the adsorption of CP to CaO_2 and decreased the surface active sites at CaO_2 surface, leading to the decrease of CP removal efficiency.

3.2.3. Initial pH value and reaction time

Effects and interactions of initial pH value and reaction time on CP removal efficiency are shown in Figs. 4(e) and (f). With the increase of initial pH value, the CP removal efficiency increased at first and then decreased, especially at a reaction time of less than 7.5 min. The pH value influenced H_2O_2 emission and CaO_2 dissolution. At low pH values, CaO_2 reagent dissolved rapidly and released H_2O_2 instantaneously, causing excessive disproportionation of H_2O_2 as presented in Eq. (9) [40]. Since H_2O_2 most likely released O_2 instead of HO• radicals, the CP removal efficiency decreased in the acidic condition (initial pH values less than 7). However, at initial pH values higher than 7, CaO_2 reagent was difficult to dissolve to generate H_2O_2, and the main reaction changed to produce $Ca(OH)_2$ and O_2 as shown in Eq. (2) [37]. With the increase of pH in alkaline conditions (initial pH values larger than 7), the production of H_2O_2 decreased, causing a decrease in CP removal efficiency (Fig. 4(e)). CaO_2 treatment was therefore, most effective at pH values around 7. It was a remarkable advantage in comparison with the conventional Fenton process with the optimum pH value around 3.

The elliptical contour plot as shown in Fig. 4(e) indicates interactions between initial pH value and reaction time. The joint effect of initial pH and reaction time promoted CP removal with a positive coefficient (+ 5.80 ± 2.66) as shown in Table 5. At higher pH values, dissolution of CaO_2 and generation of H_2O_2 and HO• radicals needed more time, thus synergistically affected the removal efficiency of CP.

The effects and interactions of CaO_2 dosage and initial pH (p-value of x_1x_2 at 0.2810), initial pH and initial CP concentration (p-value of x_2x_4 at 0.9631), and reaction time and initial CP concentration (p-value of x_3x_4 at 0.1767) are shown in Fig. 6. As shown in Figs. 6(a), (c), and (e), the effect of each variable showed the same trend as described in section 3.2 and shown in Fig. 4. The interactions of these variables were insignificant and were negligible with a circular contour of response surfaces as shown in Figs. 6(b), (d) and (f).

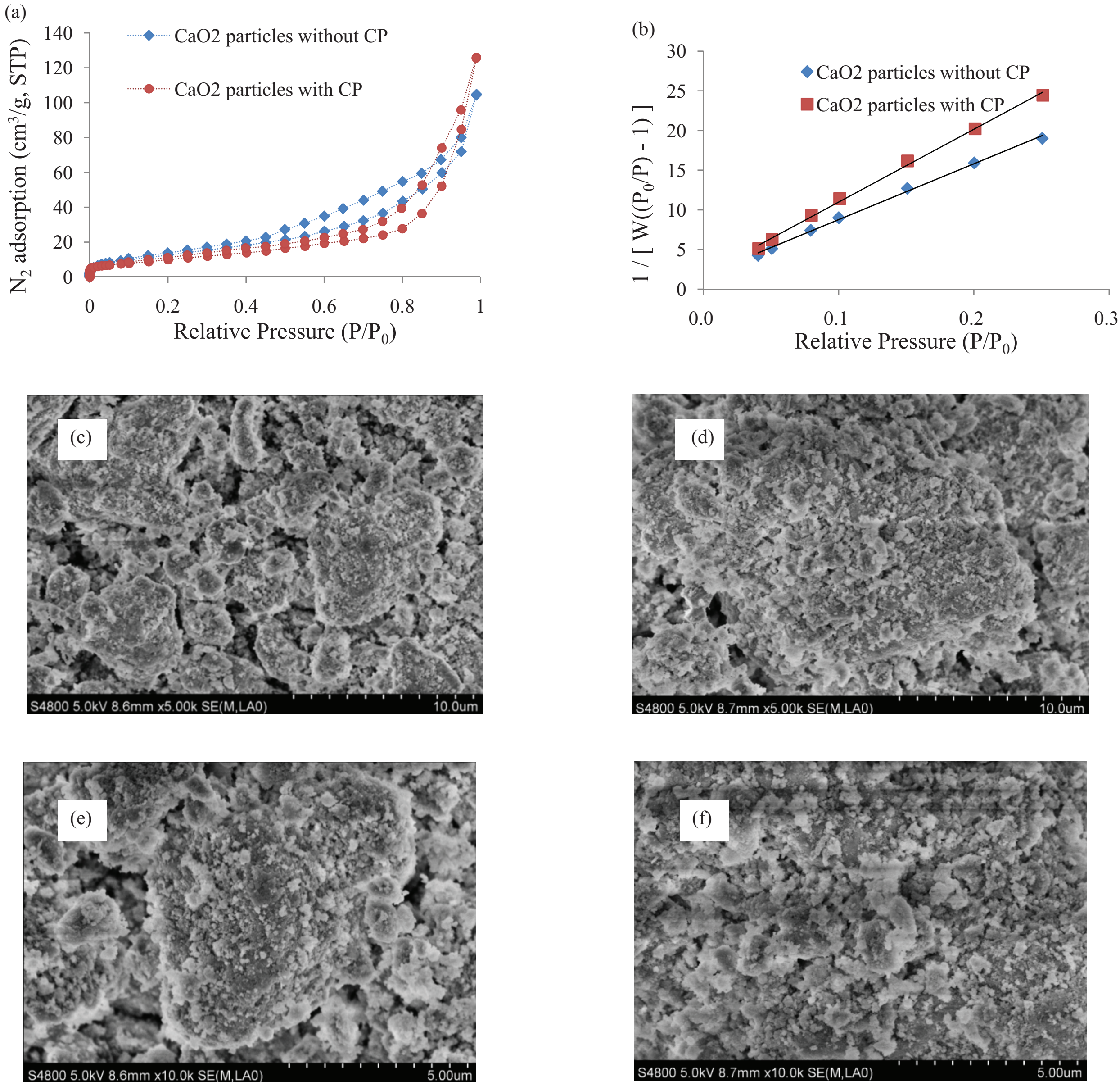

Fig. 5. N_2 adsorption-desorption isotherms (a) and BET curves (b) of CaO_2 particles with and without the addition of 0.6 mM of CP; SEM images of CaO_2 particles without the addition of CP of (c) 10 µm, (e) 5 µm and with 0.6 mM of CP of (d) 10 µm, (f) 5 µm. Experimental conditions: CaO_2 dosage at 0.1 g L^{-1} with pH unadjusted stirring for 1 min.

Based on the above, efficient CP removal was achieved due to the coupled effects of oxidation and adsorption in CaO_2 treatment. With the addition of CaO_2, H_2O_2 was generated according to Eq. (1). Since the purity of commercial CaO_2 reagent is usually less than 80% as shown in Fig. S1, various mineral impurities presenting in CaO_2 reagent may catalyze the generation of HO• from H_2O_2 [41]. The existing metal ions in CaO_2 reagent and H_2O_2 releasing from CaO_2 could function as Fenton-like reagent and promote CP removal. Moreover, the removal of CP was promoted by adsorption of CaO_2 and $Ca(OH)_2$ formed as shown in Eqs. (1) and (2). As the reaction progress, the specific surface area of CaO_2 particles decreased as shown in Figs. 5(a) and 5(b) due to the aggregation of several particles as shown in Figs. 5(c)–(f). The surface hydroxyl groups that behaved as active sites also decreased with the decrease of surface area of CaO_2 particles [41].

3.3. Optimization of influencing factors for CP removal efficiency

In optimization, the desired goal was to achieve the maximum CP removal efficiency within the experimental range of the variables (CaO_2 dosage, reaction time, and initial CP concentration). The initial pH value was selected to be 7 while practically considering reducing the cost of reagents in adjusting pH values. As illustrated in Table 6, the optimum values of the variables according to Eq. (6) were CaO_2 dose of 3.43 g L^{-1}, initial pH value of 7, reaction time of 17.34 min, and initial CP

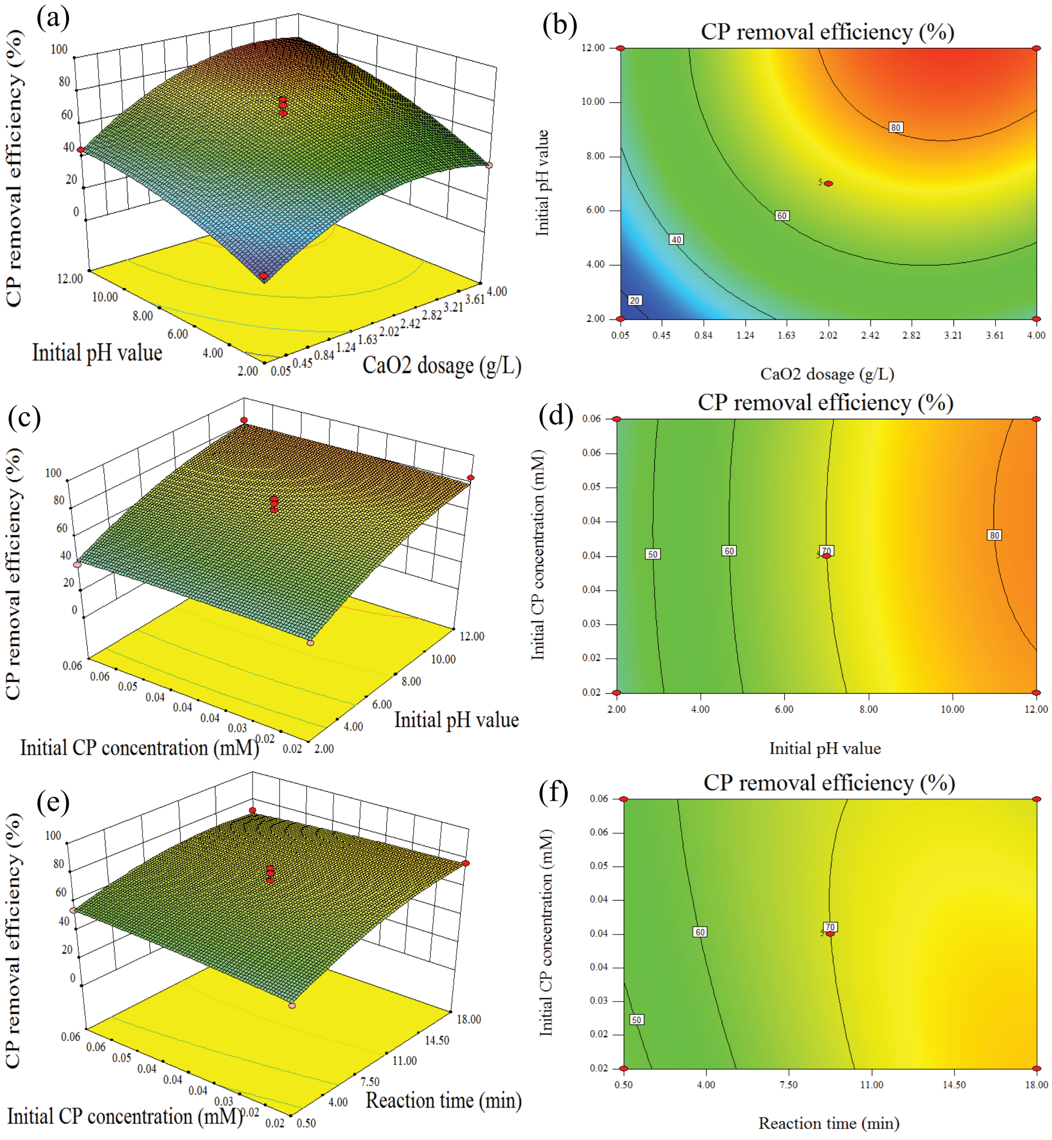

Fig. 6. Response surface plots (a, c, and e) and contour plots (b, d, and f) for effects of the CaO_2 dosage and initial pH value (a and b), initial pH value and initial CP concentration (c and d), and reaction time and initial CP concentration (e and f) on CP removal efficiency while the other variables kept at central level (CaO_2 dosage at 2.02 g L^{-1}, initial pH at 7, reaction time at 9.25 min, and initial CP concentration at 0.04 mM).

Table 6
Optimum operating conditions of the process variables for CP removal efficiency

Parameter	Goal	Lower limit	Upper limit	Value
CaO_2 dosage (g L^{-1})	In range	0.05	4	3.43
Initial pH value	Target = 7	2	12	7
Reaction time (min)	In range	0.5	18	17.34
Initial CP concentration (mM)	In range	0.02	0.06	0.03
CP removal efficiency (%)	Maximum	18.29	90.6	94.97
Desirability				1.000

concentration of 0.03 mM. At these optimized conditions, the model predicted 95.0% of CP removal efficiency.

Additional experiments were performed under the projected optimal conditions based on the results given in Table 6 so as to confirm the validity of the optimization procedure. In the experiments, the CP removal efficiency was 94.2% ± 1.7% which was closer to the proposed one by the model (95.0% of CP removal efficiency), meaning that the optimization procedure was valid.

3.4. Change in UV absorbance

The change in UV absorbance can imply change in chemical structures [37]. The UV absorption spectra of CP samples during treatment are shown in Fig. 7.

Changes in absorbance were in the range of $235 < \lambda < 250$ nm as shown in Fig. 7. With the increase of reaction time, an increase from 0 to 2 min and a decrease from 2 to 4 min and an increase from 4 to 12 min occurred. UV absorbance in the range of 230–280 nm was an indicator of sp^2-hybridized carbon (e.g., alkene carbon, alcohol carbon, keto-carbon, and acyl carbon) [42]. The initial increase followed by a sharp decrease in absorbance in this specific wavelength range signaled formation of the sp^2-hybridized carbon at first and then a considerable removal of the same during treatment.

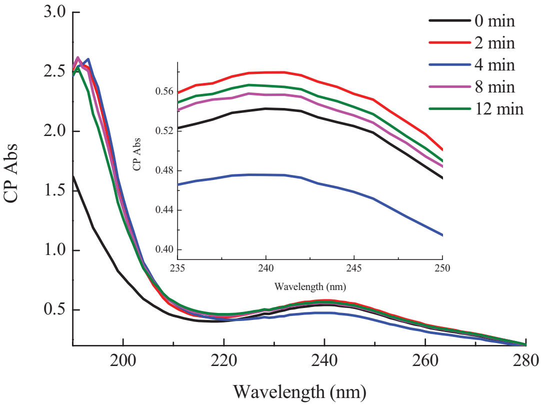

Fig. 7. UV absorption spectra at 190 to 280 nm of CP contaminated water samples during CaO_2 oxidation. Experimental conditions: the initial pH was 7 and the initial CP concentration was 0.06 mM with a CaO_2 dosage of 0.08 g L^{-1}.

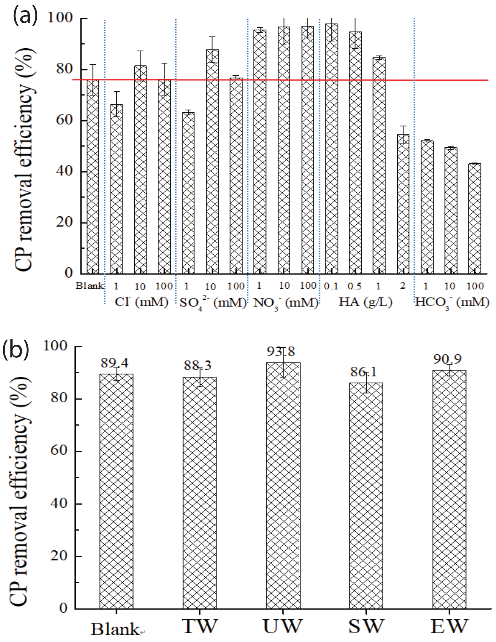

Fig. 8. Effects of inorganic anions and HA at various concentrations on CP removal during CaO_2 treatment ((a) unadjusted pH, CaO_2 of 3.43 g L^{-1}, CP at 0.03 mM, and reaction time for 10 min), and effects of water matrix on CP removal (b) unadjusted pH, CaO_2 of 3.43 g L^{-1}, CP at 0.03 mM, and reaction time for 18 min).

The stability and potency of GCs could be changed by the modification of their perhydrocyclopentanophenanthrene structures, such as epoxidation at alkene carbon, substitution at alcohol carbon, and esterification at keto-carbon and/or acyl carbon [43]. In this study, the change in absorbance may indicate these variants in the molecular structure and activities of GCs during CaO_2 treatment. Further research on the change of GC activities during oxidation should be conducted more systematically.

3.5. Influences of background water matrix

The influence of commonly existing inorganic anions and dissolved organic matters (such as HA) in water matrix on CP removal were investigated and the findings were as shown in Fig. 8(a). Compared with Cl^-, SO_4^{2}, and NO_3^-, the presence of HCO_3^- significantly inhibited CP removal. There was a possibility of Cl^-, HCO_3^-, and SO_4^{2-} competing with CP for HO• radical, resulting to decrease in CP removal efficiencies [44]. HA can improve CP removal efficiencies by adsorption [36]. On the other hand, HA could also compete with CP for HO• during CaO_2 oxidation, causing the decrease in CP removal efficiencies [36].

Based on the effects of each individual component in water matrix on CP removal, evaluation of CP removal in four complex and real media were conducted and shown in Fig. 8(b). The main parameters determined from the four real water samples are shown in Table 1. Within the four real water matrices tested, the highest removal efficiency was obtained in UW, followed by the EW, while the SW led to much lower removal efficiency. According to the quality parameter values shown in Table 1, the concentration of HCO_3^- in matrices followed the order SW > TW > EW > UW. Therefore, more HCO_3^- existing in water matrices, the lower the CP removal efficiencies obtained, meaning that HCO_3^- played an important role in CP removal by CaO_2. Although, HCO_3^- could significantly inhibit the CP removal, no obvious decrease of CP removal efficiency occurred in real water matrix compared with the blank (Fig. 8(b)). This indicates that other constituents in real matrices may play a positive effect on CP removal. For example, the presence of metal ions in water matrix can participate in Fenton-type reactions and promote the CP removal [36]. Therefore, CaO_2 treatment was suitable for CP removal in common water matrix.

4. Conclusion

CaO_2 treatment is efficient in CP removal. The operating factors of CaO_2 dosage, initial pH value, reaction time, and initial CP concentration influenced the efficiency of CP removal during CaO_2 treatment. A model was developed to accurately predict CP removal efficiencies at different operating conditions.

Effects and interactions of different variables were evaluated by RSM. With CaO_2 dose increased, the CP removal efficiency increased at first and then decreased. The effect of initial CP concentration on CP removal efficiency was dependent on CaO_2 dosage because of the aggregation of CaO_2 particles at high CP concentration and CaO_2 dosage. The application of CaO_2 enabled the adjustment of the reaction rate at a wide pH range and was most effective at near-neutral pH values.

The optimum operating conditions were a CaO_2 dose of 3.43 g L^{-1}, initial pH value of 7, reaction time of 17.34 min, and initial CP concentration of 0.03 mM. At the optimized conditions, the CP removal efficiency achieved 94.18% ± 1.72%. The change in absorbance indicated the variants in CP molecular structure and activities of GCs during CaO_2 treatment.

The presence of HCO_3^- in real water matrix can significantly inhibit CP removal. However, with the existence of other constituents, no obvious decrease of CP removal efficiency occurred in real water matrix compared with in ultrapure water. Therefore, CaO_2 treatment was suitable for CP removal in common water matrix.

Acknowledgments

This work was supported by the Fundamental Research Funds for the Central Universities (Grant no. 2232018D3–31), National Natural Science Foundation of China (Grant no. 51708096), the Opening Project of Shanghai Key Laboratory of Atmospheric Particle Pollution and Prevention (LAP^3) and China Postdoctoral Science Foundation (Grant no. 2017M611423). All the financial supports are gratefully acknowledged.

Conflict of interest

The authors declare no competing financial interest and human conflicts.

References

[1] S. Kugathas, J.P Sumpter, Synthetic glucocorticoids in the environment: first results on their potential impacts on fish, Environ. Sci. Technol., 45 (2011) 2377–2383.
[2] H. Chang, J. Hu, B. Shao, Occurrence of natural and synthetic glucocorticoids in sewage treatment plants and receiving river waters, Environ. Sci. Technol., 41 (2007) 3462–3468.
[3] A. Jia, S.M. Wu, K.D. Daniels, S.A Snyder, Balancing the budget: accounting for glucocorticoid bioactivity and fate during water treatment, Environ. Sci. Technol., 50 (2016) 2870–2880.
[4] BNF 2006, British National Formulary (BNF52), British Medical Association and Royal Pharmaceutical Society of Great Britain, September 2006, pp. 916.
[5] Z. Fan, S. Wu, H. Chang, J. Hu, Behaviors of glucocorticoids, androgens and progestogens in a municipal sewage treatment plant: comparison to estrogens, Environ. Sci. Technol., 45 (2011) 2725–2733.
[6] J. Brausch, K. Connors, B. Brooks, G. Rand, In: D.M. Whitacre, Human pharmaceuticals in the aquatic environment: a review of recent toxicological studies and considerations for toxicity testing, Rev. Environ. Contam. Toxicol., 218 (2012) 1–99.
[7] C.A. Lalone, D.L. Villeneuve, A.W. Olmstead, E.K. Medlock, M.D. Kahl, K.M. Jensen, E.J. Durhan, E.A. Makynen, C.A. Blanksma, J.E. Cavallin, L.M. Thomas, S.M. Seidl, S.Y. Skolness, L.C. Wehmas, R.D. Johnson, G.T. Ankley, Effects of a glucocorticoid receptor agonist, dexamethasone, on fathead minnow reproduction, growth, and development, Environ. Toxicol. Chem., 31 (2012) 611–622.
[8] M. Schriks, J.A. van Leerdam, S.C. van der Linden, B. van der Burg, A.P. van Wezel, P. de Voogt, High-Resolution mass spectrometric identification and quantification of glucocorticoid compounds in various wastewaters in the Netherlands, Environ. Sci. Technol., 44 (2010) 4766–4774.
[9] N. Creusot, S. Aït-Aïssa, N. Tapie, P. Pardon, F. Brion, W. Sanchez, E. Thybaud, J.M. Porcher, H. Budzinski, Identification of synthetic steroids in river water downstream from pharmaceutical manufacture discharges based on a bioanalytical approach and passive sampling, Environ. Sci. Technol., 48 (2014) 3649–3657.
[10] T. Isobe, K. Sato, K. Joon-Woo, S. Tanabe, G. Suzuki, K. Nakayama, Determination of natural and synthetic glucocorticoids in effluent of sewage treatment plants using ultrahigh performance liquid chromatography-tandem mass spectrometry, Environ. Sci. Pollut. Res., 22 (2015) 14127–14135.
[11] M. Pedrouzo, F. Borrull, R.M. Marcé, E. Pocurull, Ultra-high-performance liquid chromatography-tandem mass spectrometry for determining the presence of eleven personal care products in surface and wastewaters, J. Chromatogr. A., 1216 (2009) 6994–7000.
[12] J. Roberts, P.A. Bain, A. Kumar, C. Hepplewhite, D.J. Ellis, A.G. Christy, S.G. Beavis, Tracking multiple modes of endocrine activity in Australia's largest inland sewage treatment plant and effluent – receiving environment using a panel of in vitro bioassays, Environ. Toxicol. Chem., 34 (2015) 2271–2281.
[13] D. Shargil, P. Fine, Z. Gerstl, I. Nitsan, D. Kurtzman, Impact of biosolids and wastewater effluent application to agricultural land on corticosterone content in lettuce plants, Sci. Total. Environ., 541 (2016) 742–749.
[14] A. Lange, G.C. Paull, T.S. Coe, Y. Katsu, H. Urushitani, T. Iguchi, T.R. Charles, Sexual reprogramming and estrogenic sensitization in wild fish exposed to ethinylestradiol, Environ. Sci. Technol., 43 (2009) 1219–1225.
[15] M. Klavarioti, D. Mantzavinos, D. Kassinos, Removal of residual pharmaceuticals from aqueous systems by advanced oxidation processes, Environ. Int., 35 (2009) 402–417.
[16] V. Kumar, A.C. Johnson, A. Trubiroha, J. Tumov, M. Ihara, R. Grabic, W. Kloas, H. Tanaka, H.K. Kroupová, The challenge presented by progestins in ecotoxicological research: a critical review, Environ. Sci. Technol., 49 (2015) 2625–2638.
[17] Z.H. Liu, Y. Kanjo. S. Mizutani, Removal mechanisms for endocrine disrupting compounds (EDCs) in wastewater treatment – physical means, biodegradation, and chemical advanced oxidation: a review. Sci. Total Environ., 407 (2009) 731–748.
[18] Y. Zhou, X. Fang, T. Wang, Y. Hu, J. Lu, Chelating agents enhanced CaO_2 oxidation of bisphenol A catalyzed by Fe^{3+} and reuse of ferric sludge as a source of catalyst, Chem. Eng. J., 313 (2017) 638–645.
[19] A. Zhang, J. Wang, Y. Li, Performance of calcium peroxide for removal of endocrine-disrupting compounds in waste activated sludge and promotion of sludge solubilization, Water. Res., 71 (2015) 125–139.
[20] Y. Xue, X. Gu, S. Lu, Z. Miao, M.L. Brusseau, M. Xu, X. Fu, X. Zhang, Z. Qiu, Q. Sui, The destruction of benzene by calcium peroxide activated with Fe(II) in water, Chem. Eng. J., 302 (2016) 187–193.
[21] S. Lu, X. Zhang, Y. Xue, Application of calcium peroxide in water and soil treatment: a review, J. Hazard. Mater., 337 (2017) 163–177.
[22] A.C. Ndjou'ou, D. Cassidy, Surfactant production accompanying the modified Fenton oxidation of hydrocarbons in soil, Chemosphere, 65 (2006) 1610–1615.
[23] B. Yang, J.J. Pignatello, D. Qu, B. Xing, Activation of hydrogen peroxide and solid peroxide reagents by phosphate ion in alkaline solution, Environ. Eng. Sci., 33 (2016) 193–199.
[24] Drugs.com U.S. Pharmaceutical Sales 2013. Available at: http://www.drugs.com/stats/top100/2013/units (Accessed on 21 May 2013).
[25] A. Amiri, M.R. Sabour, Multi-response optimization of Fenton process for applicability assessment in landfill leachate treatment, Waste. Manage., 34 (2014) 2528–2536.
[26] A.J. Jafari, B. Kakavandi, R.R. Kalantary, H. Gharibi, A. Asadi, A. Azari, A.A. Babaei, A. Takdastan. Application of mesoporous magnetic carbon composite for reactive dyes removal: process optimization using response surface methodology, Korean J. Chem. Eng., 33 (2016) 2878–2890.

[27] M. Ahmadi, B. Kakavandi, S. Jorfi, M. Azizi, Oxidative degradation of aniline and benzotriazole over PAC@$Fe^{II}Fe_2^{III}O_4$: a recyclable catalyst in a heterogeneous photo-Fenton-like system, J. Photochem. Photobiol., A, 336 (2017) 42–53.

[28] A. Takdastan, B. Kakavandi, M. Azizi, M. Golshan, Efficient activation of peroxymonosulfate by using ferroferric oxide supported on carbon/UV/US system: a new approach into catalytic degradation of bisphenol A, Chem. Eng. J., 331 (2018) 729–743.

[29] D. Bingöl, S. Veli, S. Zor, U. Özdemir, Analysis of adsorption of reactive azo dye onto $CuCl_2$ doped polyaniline using Box-Behnken design approach, Synth. Met., 162 (2012) 1566–1571.

[30] K.K. Doddapaneni, R. Tatineni, R. Potumarthi, L.N. Mangamoori, Optimization of media constituents through response surface methodology for improved production of alkaline proteases by Serratia rubidaea, J. Chem. Technol. Biotechnol., 82 (2007) 721–729.

[31] R. Myers, D. Montgomery, Response surface methodology: process and product optimization using designed experiments, 2nd Ed.; Wiley: New York, USA, 2002; ISBN 978–1-118–21047–5.

[32] C. García-Gómez, J.A. Vidales-Contreras, J. Nápoles-Armenta, P. Gortáres-Moroyoqui, Optimization of phenol removal using Ti/PbO_2 anode with response surface methodology, J. Environ. Eng., 142 (2016) 04016004.

[33] A.M. Joglekar, A.T. May, Product excellence through design of experiments, Cereal. Foods. World., 32 (1987) 857–868.

[34] M. Behbahani, M.R. Alavi Moghaddam, M. Arami, Techno-economical evaluation of fluoride removal by electrocoagulation process: optimization through response surface methodology, Desalination, 271 (2011) 209–218.

[35] A.J. Bora, S. Gogoi, G. Baruah, R.K. Dutta, Utilization of co-existing iron in arsenic removal from groundwater by oxidation-coagulation at optimized pH, J. Environ. Chem. Eng., 4 (2016) 2683–2691.

[36] A. Zhang, Y. Li, Removal of phenolic endocrine disrupting compounds from waste activated sludge using UV, H_2O_2, and UV/H_2O_2 oxidation processes: effects of reaction conditions and sludge matrix, Sci. Total Environ., 493 (2014) 307–323.

[37] X. Zhang, X. Gu, S. Lu, Z. Miao, M. Xu, X. Fu, Z. Qiu, Q. Sui, Degradation of trichloroethylene in aqueous solution by calcium peroxide activated with ferrous ion, J. Hazard. Mater., 284 (2015) 253–260.

[38] M. Sleiman, D. Vildozo, C. Ferronato, J.M. Chovelon, Photocatalytic degradation of azo dye Metanil Yellow: optimization and kinetic modeling using a chemometric approach, Appl. Catal. B – Environ., 77 (2007) 1–11.

[39] A.M. Salehi, G.M.K. Yaghmaeian, Preparation, characterization and catalytic activity of a novel mesoporous nanocrystalline MgO nanoparticle for ozonation of acetaminophen as an emerging water contaminant, Chem. Eng. J., 310 (2017) 157–169.

[40] M. Arienzo, Degradation of 2, 4, 6 - trinitrotoluene in water and soil slurry utilizing a calcium peroxide compound, Chemosphere, 40 (2000) 331–337.

[41] A. Zhang, X. Shen, X. Yin, X. Li, Y. Liu, Application of calcium peroxide for efficient removal of triamcinolone acetonide from aqueous solutions: mechanisms and products, Chem. Eng. J., 345 (2018) 594–603.

[42] P. Westerhoff, P. Chao, H. Mash, Reactivity of natural organic matter with aqueous chlorine and bromine, Water. Res., 38 (2004) 1502–1513.

[43] W. Sandra, C.S. Leopold, R.H. Guy, Bioavailability and bioequivalence of topical glucocorticoids, Eur. J. Pharm. Biopharm., 68 (2008) 453–466.

[44] Y. Zhang, J. Zhang, Y. Xiao, V.W.C. Chang, T.T. Lim, Kinetic and mechanistic investigation of azathioprine degradation in water by UV, UV/H_2O_2 and UV/persulfate, Chem. Eng. J., 302 (2016) 526–534.

[45] N. Creusot, S. Ait-Aissa, N. Tapie, P. Pardon, F. Brion, W. Sanchez, E. Thybaud, J.M. Porcher, H. Budzinski, Identification of synthetic steroids in river water downstream from pharmaceutical manufacture discharges based on a bioanalytical approach and passive sampling, Environ. Sci. Technol., 48 (2014) 3649–3657.

[46] A.L. Carlie, L.V. Daniel, W.O. Allen, K.M. Elizabeth, D.K. Michael, M.J. Kathleen, J.D. Elizabeth, A.M. Elizabeth, A.B. Chad, E.C. Jenna, M.T. Linnea, M.S. Sara, Y.S. Sarah, C.W. Leah, D.J. Rodney, T.A. Gerald, Effects of a glucocorticoid receptor agonist, dexamethasone, on fathead minnow reproduction, growth, and development, Environ. Toxicol. Chem., 31 (2012) 611–622.

[47] S. Kugathas, R.J. Williams, J.P. Sumpter, Prediction of environmental concentrations of glucocorticoids: the River Thames, UK, Environ. Int., 40 (2012) 15–23.

[48] T. Anumol, S. Merel, B. Clarke, S. Snyder, Ultra high performance liquid chromatography tandem masss pectrometry for rapid analysis of trace organic contaminants in water, Cent. Eur. J. Chem., 7 (2013) 1–14.

[49] H. Chang, J.Y. Hu, B. Shao, Occurrence of natural and synthetic glucocorticoids in sewage treatment plants and receiving river waters, Environ. Sci. Technol., 41 (2007) 3462–3468.

[50] P.A. Bain, M. Williams, A. Kumar, Assessment of multiple hormonal activities in wastewater at different stages of treatment, Environ. Toxicol. Chem., 33 (2014) 2297–2307.

[51] A. Jia, B.I. Escher, F.D.L. Leusch, J.Y.M. Tang, E. Prochazka, B.F. Dong, E.M. Snyder, S.A. Snyder, In vitro bioassays to evaluate complex chemical mixtures in recycled water, Water. Res., 80 (2015) 1–11.

[52] A.C. Mehinto, A. Jia, S.A. Snyder, B.S. Jayasinghe, N.D. Denslow, J. Crago, D. Schlenk, C. Menzie, S.D. Westerheide, F.D.L. Leusch, K.A. Maruya, Interlaboratory comparison of in vitro bioassays for screening of endocrine active chemicals in recycled water, Water. Res., 83 (2015) 303–309.

[53] Z.L. Fan, S.M. Wu, H. Chang, J.Y. Hu, Behaviors of glucocorticoids, androgens and progestogens in a municipal sewage treatment plant: comparison to estrogens, Environ. Sci. Technol., 45 (2011) 2725–2733.

[54] A. Piram, A. Salvador, J.Y. Gauvrit, P. Lanteri, R. Faure, Development and optimisation of a single extraction procedure for the LC/MS/MS analysis of two pharmaceutical classes residues in sewage treatment, plant. Talanta, 74 (2008) 1463–1475.

[55] S.C. Van der Linden, M.B. Heringa, H.Y. Man, E. Sonneveld, L.M. Puijker, A. Brouwer, B. Van der Burg, Detection of multiple hormonal activities in wastewater effluents and surface water, using a panel of steroid receptor CALUX bioassays, Environ. Sci. Technol., 42 (2008) 5814–5820.

[56] M. Schriks, J.A. van Leerdam, S.C. van der Linden, B. van der Burg, A.P. van Wezel, P. de Voogt, High-Resolution mass spectrometric identification and quantification of glucocorticoid compounds in various wastewaters in the Netherlands, Environ. Sci. Technol., 44 (2010) 4766–4774.

[57] G. Suzuki, K. Sato, T. Isobe, H. Takigami, A. Brouwer, K. Nakayama, Detection of glucocorticoid receptor agonists in effluents from sewage treatment plants in Japan, Sci. Total. Environ., 527 (2015) 328–334.

[58] P. Macikova, K.J. Groh, A.A. Ammann, K. Schirmer, M.J.F. Suter, Endocrine disrupting compounds affecting corticosteroid signaling pathways in Czech and Swiss Waters: Potential Impact on Fish, Environ. Sci. Technol., 48 (2014) 12902–12911.

Supplementary information

Table S1
Concentrations of GCs in water samples from various countries

Glucocorticoid	Type of samples	Country	Concentration (ng/L)	References
Prednisolone	Industrial and hospital wastewater	France	250–2,000	[45]
Dexamethasone	Wastewater of pharmaceutical factory	France	10,000	[46]
Dexamethasone	Effluent of an industrial WWTP	France	Up to 23,000	[45]
Prednisone	River water		Up to 300	
Dexamethasone			1–2,900	
6α-methylprednisolone			50–1,260	
Total GC levels	River thames	UK	30–850	[47]
Prednisone	WWTP effluent in Arizona	USA	20	[48]
Hydrocortisone			7	
Total GC levels	45 river samples in Beijing region	China	Up to 52	[49]
Total GC levels	Municipal wastewater	Australia	Up to 81	[50]
Total GC levels	WWTP secondary effluent and effluent after ozonation or chlorination	USA	16–24	[51]
Total GC levels	WWTP secondary effluent subject to ozonation, microfiltration, reverse osmosis, or ultraviolet	USA	<52–90	[52]
Total GC levels	WWTP influents	China	42 ± 2	[53]
	WWTP effluents		0.7 ± 0.1	
	Dehydrated sludge samples		1.2 ± 0.3	
Prednisone	Influents in sewage treatment plants	China	2.6 ± 2.1	[49]
Prednisolone			3.0 ± 1.6	
Cortisone			30 ± 21	
Cortisol			39 ± 26	
Dexamethasone			1.2 ± 0.7	
6α-methylprednisolone			0.62 ± 0.65	
Betamethasone and	Pierre Benite influents/effluents STP	France	15/7	[54]
dexamethasone			<0.007/3	
Budesonide			174/229	
Cortisone			53/63	
Cortisol			7/5	
Flunisolide			0.3/11	
Fluocinolone acetonide			31/30	
Triamcinolone			40/3	
Triamcinolone acetonide				
Total GC levels	Surface water	Netherlands	0.39–1.3	[55]
	Effluents		11–243	
Cortisol	Hospital wastewater	Netherlands	275–301	[56]
Cortisone			381–472	
Prednisone			117–545	
Prednisolone			315–1918	
Triamcinolone acetonide			14–41	
Total GC levels	STP effluents	Japan	<3.0–78	[57]
Total GC levels	River water	Switzerland	<LOD-2.6	[58]
	Treated wastewater		19–37	
	Untreated wastewater		78–542	

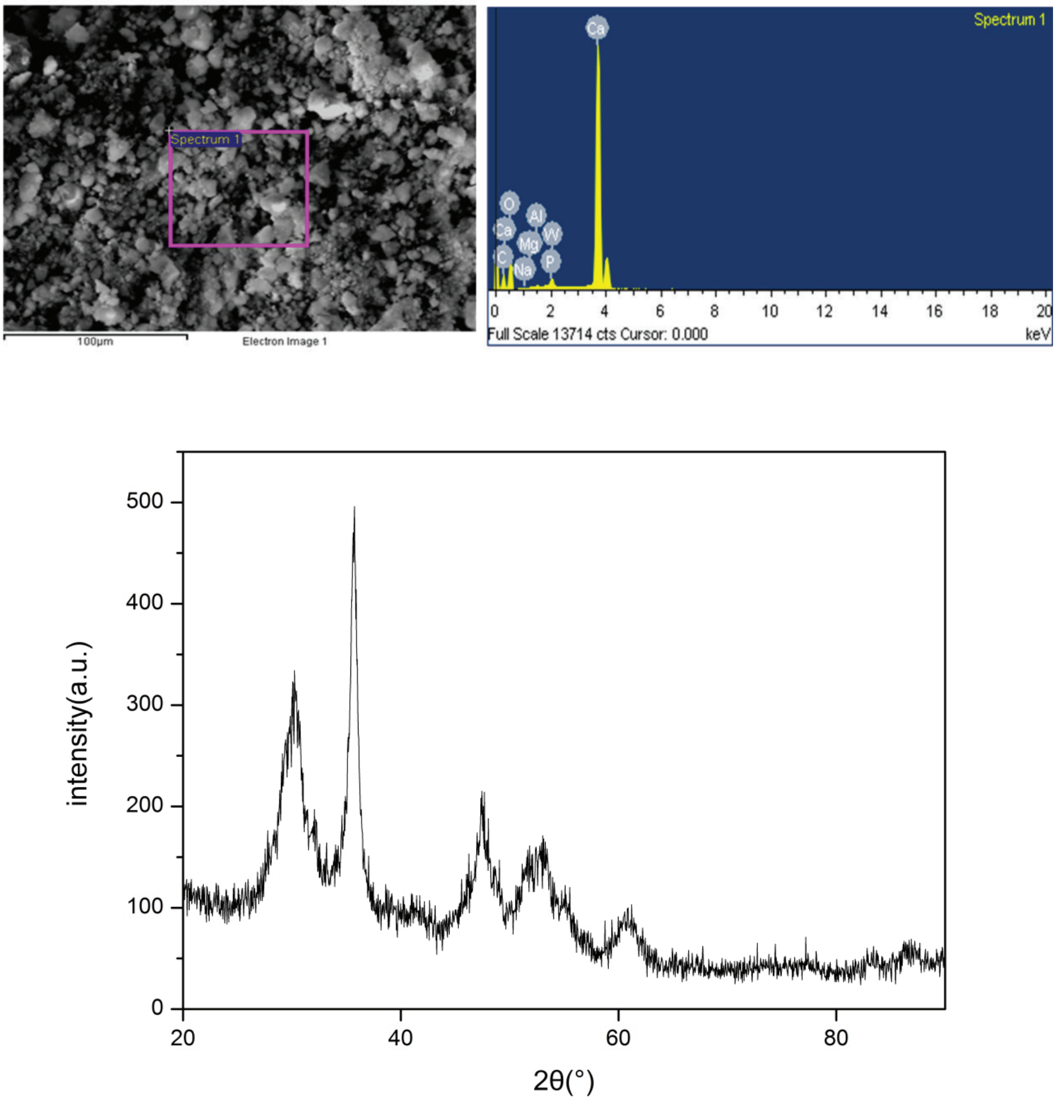

Fig. S1. Size and elemental components of calcium peroxide analyzed by SEM-EDS and crystalline phase of calcium peroxide analyzed by XRD.